Seismic Performance of Reinforced Concrete Columns With Spandrel Walls Retrofitted Using CES System

Juan Jose CASTRO, Ryo NOMURA & Hiroshi KURAMOTO
Osaka Universisy, Japan

Takashi TAGUCHI & Takashi KAMIYA
Yahagi Construction Co., Ltd., Japan

SUMMARY:
This paper presents the seismic performance of existing reinforced concrete columns with spandrel walls retrofitted by the CES outer frame retrofit system. This retrofit system consists of steel frame and fiber reinforced concrete externally attached to the exiting reinforced concrete columns.
A total of three specimens, one without retrofitting and the other two with variations in the amount of the attached steel reinforcements, were tested.
The test results showed that, the CES retrofit system improves the seismic behavior of the columns with spandrel walls. Also it was proved that the ultimate strength of existing columns can be properly estimated by the superimposed strength theory.

Keywords: Retrofitting, CES Columns, Fiber, Static loading test, Deformation capacity

1. INTRODUCTION

In recent years the seismic retrofitting of existing structures, designed under old standards, has been one of the alternatives for mitigating against destructives earthquakes.

Enlarging the cross section of existing structural members, steel or carbon fiber jacketing for columns and beams, or attaching new shear walls or steel braces to the existing structural system are among the most common solutions for seismically deficient reinforced concrete structures. In some cases the new steel braces are placed on the exterior face of the buildings, to keep them in operation while the retrofit works are carried out. However when the braces are placed outside of the building, they become an obstacle for good illumination, which is a condition in case of school buildings. In this sense, a steel-fiber reinforced concrete composite retrofit system was proposed (Taguchi, Kuramoto et. al, 2007), using the column encased system (CES) as shown in Fig. 1.1.

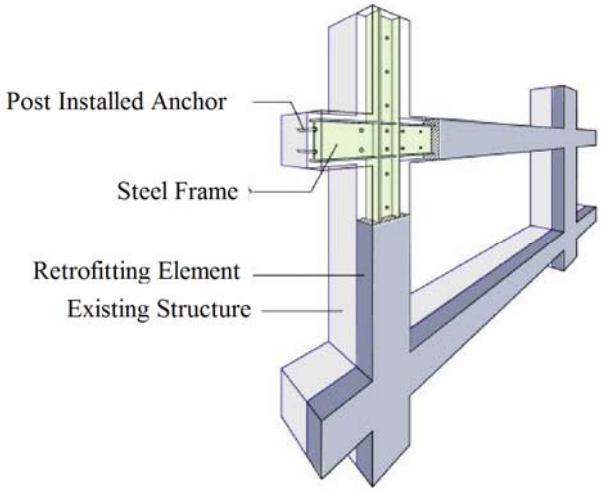

Figure 1.1 Outline of the CES outer frame retrofit system

The CES structural system is a steel-concrete composite structure, without reinforcing bars (Kuramoto et. al, 2000). According previous researches using fiber reinforced concrete (FRC), with plastic fibers, the CES system showed restoring force characteristics comparable to those of the conventional steel reinforced concrete (SRC) structures (Kuramoto et. al, 2002).

When CES system is used for retrofitting works, the steel element is attached to the existing structure by bonded anchors and after that the concrete with fibers is placed. Since no reinforcing bars are placed, the retrofitting works become very simple.

Previous experiments using this CES system, with the attached steel amount ratio, the failure mode (bending or shear), the shear span ratio and variable axial force as parameters were carried out. The test results showed that not only initial stiffness but also the ultimate strength as well as the deformation capacity can be improved with this retrofit system.

Quite often specially in condominium buildings in Japan, there are exterior walls that need to accommodate doors or windows, therefore the effective height of column over which it can be bend is restricted by the adjacent walls. It its very well known that the spandrel wall can produce an effect of short column when seismic forces are acting, then it can leads to the collapse of the structure due to shear failure.

This research presents the structural behavior of columns having spandrel walls, with and without retrofit, and the influence of the spandrel walls on the columns retrofitted by the CES system. Also a suitable formulation to estimate the ultimate strength of retrofitted columns is presented.

2. EXPERIMENTAL PROCEDURE

2.1 Test Specimens

Three specimens 1:2 scale, one without retrofitting, and the other two with variations on the amount steel frame used for the retrofitting element, were constructed and tested. The geometry and dimensions of specimens are shown in Fig. 2.1 and Table 2.1.

The column section was 400mm x 400mm with a height of 1600mm. The spandrel walls attached to the top and bottom of the column were 470mm in length, 400mm height and 80mm width. Therefore considering the confinement they provide to the column, the shear span ratio was 1.0.

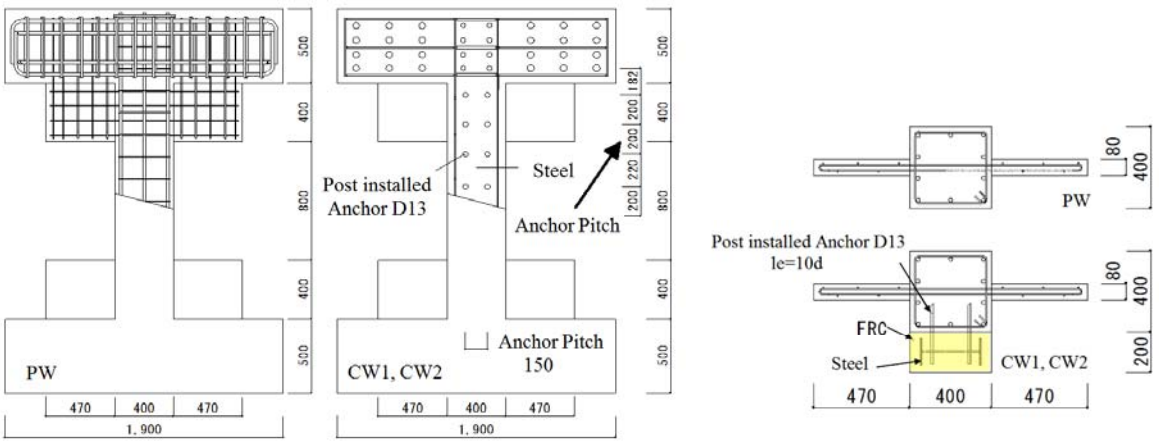

(a) Elevation (b) Section

Figure 2.1 Geometry and dimensions for test specimens

Specimen PW without retrofitting, with 10 main bars of 19 mm in diameter and the lateral reinforcement of 6 mm placed at 150 mm was designed to have shear failure. In the case of Specimen CW1, the section of the attached retrofitting element was 200mm x 400mm with H-300x130x6.5x9 steel element placed inside. On the other hand for Specimen CW2 the retrofitting element section was same as Specimen CW1, but the steel element section was increased to H-300x130x10x15. Post installed anchors of 13mm were used to fix the steel element to the existing column, where the bonded length was 10 times the anchor bar diameter (130mm).

The concrete used for the existing column had a design nominal strength of 15N/mm^2, which represents the concrete strength used in the old buildings in Japan.

Table 2.1 Outline of the test specimens

Specimens		PW	CW1	CW2
Outline		Without Retrofitting	Retrofitting	
			Standard	Over reinforced
Failure mode of existing structure		Shear failure		
Column inner height H_0(mm)		1600		
Shear span ratio M/QD		1.0		
Existing column	Concrete	Normal concrete		
	Section b x D (mm)	400 x 400		
	Column main bars	10-D19 (SD295A)		
	Column hoops	2-D6@150 (SD295A)		
	Wall reinforcing bars	Single layer D6 (SD295A)		
CES retrofitting element	Concrete		Fiber reinforced concrete	
	Section b x D (mm)		200 x 400	
	Steel section		H-300 x 130 x 6.5 x 9 (SN400B)	H-300 x 130 x 10 x 15 (SN400B)
Axial force ratio		0.2		

For the fabrication process of specimens, after the concrete hardening the column surface was roughened as shown if Photo 2.1, and then the anchor bolts were fixed using epoxy resins. Finally after set the steel element, the fiber reinforced concrete was placed to form the strengthening element.

Photo 2.1 Concrete roughening works

Photo 2.2 Fiber for FRC

2.2 Materials

The mechanical properties of the steel bars of the existing column and the steel of the retrofitting element are shown in Tables 2.2 and 2.3 respectively. Also the concrete mix proportions used for the normal concrete and FRC, as well as their mechanical properties are shown in Table 2.4 to Table 2.5 respectively.

The fiber type used for the retrofitting element concrete mix was polyvinyl alcohol type with 0.66mm diameter and 30 mm length, with fiber contents of 1% per cubic meter of concrete. See Photo 2.2. Also for the FRC, limestone was used improve the concrete fluidity.

Table 2.2 Column reinforcing bars properties

Material	Yield Strength N/mm^2	Tensile Strength N/mm^2	Young Coef. N/mm^2	Use
D6 (SD295A)	309.9	483.5	187.2	Hoops
D19 (SD295A)	345.2	517.3	198.1	Main bars

Table 2.3 Steel properties

Material	Yield Strength N/mm^2	Tensile Strength N/mm^2	Young Coef. N/mm^2	Use
PL6.5 (SN400B)	354.1	430.2	193.7	CW1 Web
PL9 (SN400B)	292.4	421.0	198.5	CW1 Flange
PL10 (SN400B)	297.9	452.1	197.8	CW2 Web
PL15 (SN400B)	270.2	450.5	198.1	CW2 Flange

Table 2.4 Concrete mix proportions

Concrete Type	W/C %	Water Kg/m^3	Cement Kg/m^3	Sand Kg/m^3	Coarse Aggregate Kg/m^3	Admixture Kg/m^3	Limestone Kg/m^3	Fiber Contents Kg/m^3	Fiber Contents Ratio
Normal	87	200	230	953	839	2.3	-	-	-
FRC	75	180	240	913	554	2.16	360	13	1.0

Table 2.5 Concrete strength

Specimen	Type of concrete	Compressive strength N/mm^2	Tensile strength N/mm^2	Use
PW	Normal concrete	18.3 (54)	1.55 (54)	Existing column
CW1	Normal concrete	18.4 (57)	2.00 (57)	Existing column
	FRC	31.4 (40)	3.14 (40)	CES retrofitting Element
CW2	Normal concrete	20.4 (61)	2.00 (57)	Existing column
	FRC	37.8 (45)	3.14 (40)	CES retrofitting Element

() represents the testing age in days

2.3 Loading System

Each of the column specimens was set under the loading apparatus shown in Fig. 2.4. These specimens were subjected to varying shear forces that were applied in a cyclic manner producing anti-symmetric bending moment distribution while being acted upon by a constant axial load. The

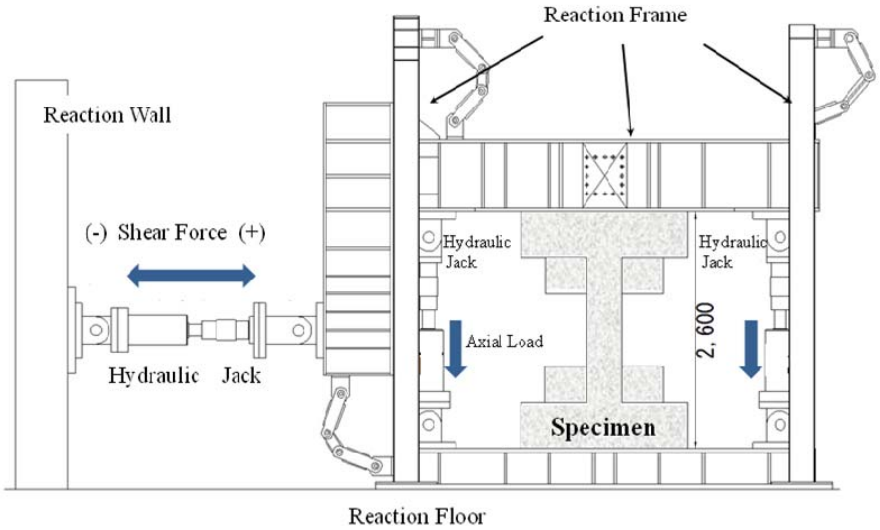

Figure 2.4 Loading apparatus

shear force was applied through the horizontal jack while the axial load was provided the two vertical jacks. The specimens were applied with a constant axial load of 586Nk which represents an axial load ratio of 0.2%, where the axial force ratio is defined as N/ b D σ_B .

For the simulation of seismic actions Specimen PW was made to drift once at a drift angle R = ± 0.002 rad. and R=± 0.004 rad., then twice at R=± 0.0067 rad., ± 0.01 rad., ± 0.015 rad., ± 0.02 rad. and R=± 0.03 rad., and again once to R=± 0.04 rad. For Specimens CW1 and CW2 the loading was extended to R=± 0.05 rad. The drift angle is defined as R=h/δ, where h is the height of the column and δ is the imposed displacement.

3. EXPERIMENTAL RESULTS

3.1. Crack Pattern

The crack patterns at the final loading stage are shown in Fig. 3.1. For convenience, in this report the side where the steel frame of the CES retrofitting element was attached is called front side, and the side of the existing column is called back side.

For Specimen PW at R=0.002 rad., shear cracks appeared at the bottom part of the column, and at the hanging wall and waist-height wall. At the loading cycle of R=0.0067 rad. on both sides of the column cracks along the main bars ware observed, together with compression failure at the joint between the column and walls.

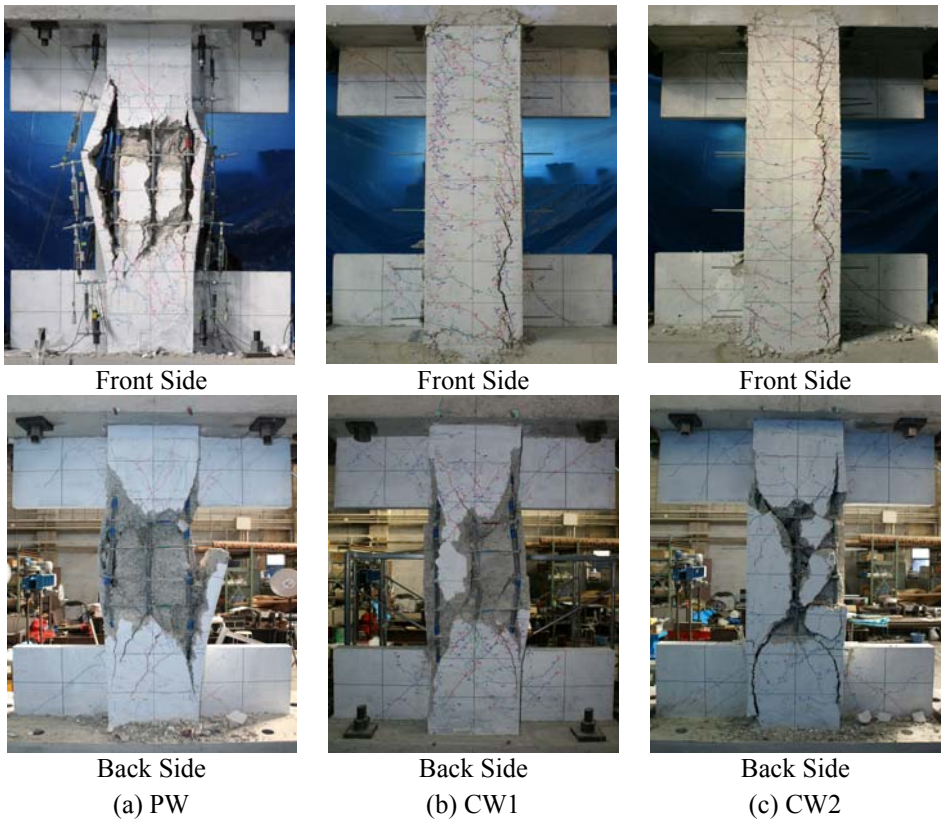

(a) PW (b) CW1 (c) CW2

Figure 3.1 Crack pattern

At R=0.01 rad., the cracks along the main bars become remarkable, especially on the middle part of the column. With the increase of the loading displacement, these cracks widened and at R=0.02 rad. concrete along the main bars spall off and they become completely exposed at the loading cycle of R=0.03 rad.

At R=0.067 rad., the concrete of hanging wall and waist height walls showed some local compression failure at the joint with the column, no further concrete degradation was observed at larger loading cycle displacements, indicating that the column was confined by the walls. Therefore, it shows that is appropriate to consider for the calculations the height of the existing column as 800 mm, which is the clear span between the hanging wall and the waist-height wall.

For Specimens CW1 and CW2 the crack patterns were very similar at the front side where the CES retrofitting element is attached. At R=0.002 rad., flexural cracks were observed at both ends of the columns and at R=0.015 rad., cracks were observed along the steel flange of the CES retrofitting element. After this with the increase of the loading cycling at R=0.04 rad., concrete spalling occurred due to the extensive cracking.

Also for both specimens at R=0.015 rad., cracks between the existing column and the retrofitting element ware recorded, but no displacement was observed even at the final loading stage. On the other hand, the back side showed almost similar patterns compared with Specimen PW.

3.2. Hysteresis Curves

The relationship of shear force applied to the column versus drift angle is presented in Fig. 3.2. For Specimen PW, the column main bars reached the yielding at R=0.004 rad., and a maximum shear force of 411.8 kN was recorded at R=0.0067 rad. After this the specimen experienced a sudden loss of the shear force carrying capacity. For this reason the experiment was stopped at the drift angle R=0.004 rad.

Specimens CW1 and CW2 with retrofitting element, presented the yielding of the existing column main bars and the attached steel at the drift angle R=0.005 rad., and the maximum shear force of 411.8kN was recorded near the drift angle R=0.01 rad. As shown in Fig. 3.1 Specimen CW1 reached the drift angle R=0.05 rad., without experiencing a sudden decrease of shear force carrying capacity.

In the case of Specimen CW2, with larger section of the H-shape steel used for the reinforcing element, compared with Specimen CW1, showed at a drift angle R=0.05 rad., the yielding of column main bars and steel. After this the shear force still continued increasing, and reached the max value at the drift angle R=0.01 rad. At the large drift angles, same as Specimen CW1, no sudden decrease of shear force carrying capacity was observed, and for the drift angle R=0.05 rad., it showed a hysteresis loops with good energy dissipation performance.

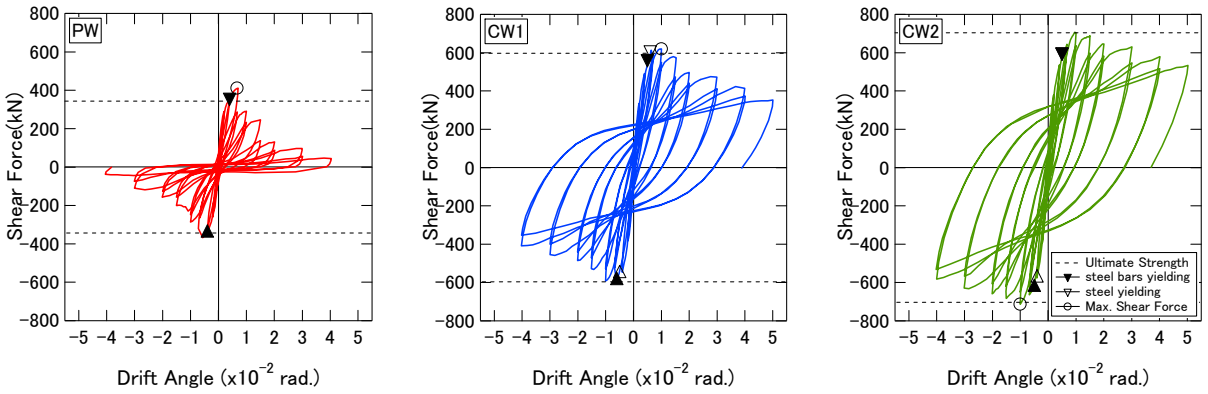

Figure 3.2 Hysteresis curves

The relationship of column shear force versus drift angle only for the CES retrofitting element is shown in Fig. 3.3. The values were obtained by subtracting from the shear force obtained for specimens CW1 and CW2 those obtained from PW without retrofit.

Specimens CW1 and CW2 presented spindle shape loops, with good energy dissipation characteristics, and showed no strength deterioration even at the large deformations. For both specimens, after the drift angle R=0.0067 rad. where the existing column showed a remarkable strength deterioration, the experimental values overtake the bending strength of the CES retrofitting element. The reason is that as the shear failure progress on the existing column, through the upper stub the axial force started to influence the CES retrofitting element therefore its bending strength also raised.

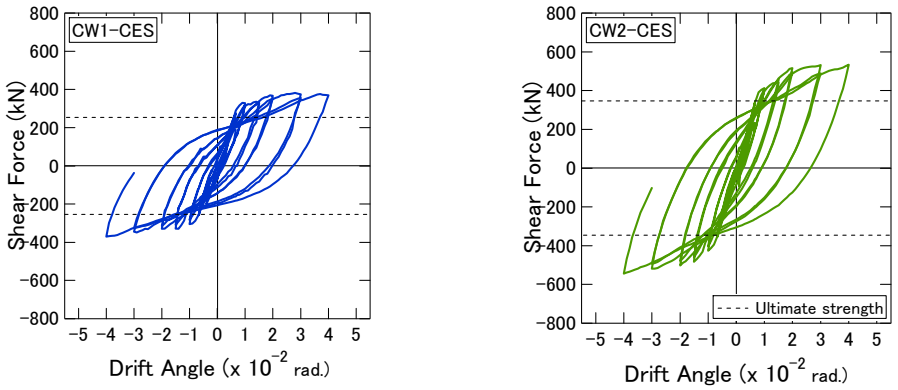

Figure 3.3 Retrofitting element hysteresis curves

3.3. Curvature Distribution

The curvature distribution of the existing column and the attached retrofitting element are shown in Fig.3.4 (a) to Fig.3.4 (c). The curvature was calculated using the data obtained from the LVDT attached to the lateral face of the column as shown in Fig. 3.4 (d).

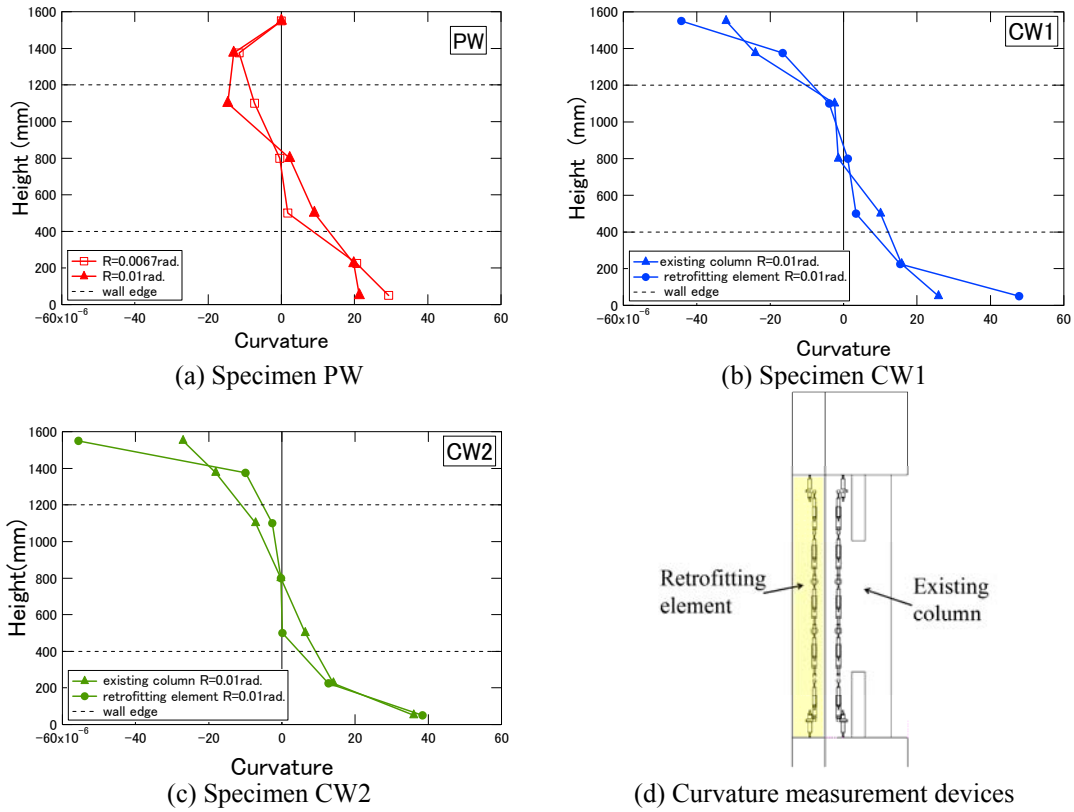

(a) Specimen PW

(b) Specimen CW1

(c) Specimen CW2

(d) Curvature measurement devices

Figure 3.4 Curvature distribution

Form the height of 400-1200mm the curvature of the existing column of Specimen PW showed larger values compared with CW1 and CW2 at the drift angle of R=0.01 rad., because of the influence of the CES retrofitting element that constrain the deformation.

For Specimens CW1 and CW2, at the height 0-400mm and 1200-1600mm, the curvature values obtained for the existing column were smaller than those obtained for the attached CES retrofitting element. This is because of the confinement given by the walls which constrain de deformation at both ends of the column. In other words the attached CES retrofitting element does not receive influence of the walls.

3.3. Stress Distribution of Column Main Bars and Steel Flange

Stress distributions on the longitudinal bars and on the steel flange of the CES retrofitting element are shown in Fig. 3.5 (a) and (b) and Fig. 3.6. The dotted lines represent the position of the edge height of the hanging wall and waist-height wall. Figure 3.7 shows the position where the strain gauges were located. The stress are plotted at the drift angle where the specimen reached the maximum shear force, that is R=0.0067 rad., for Specimen PW and R=0.01 rad. for Specimens CW1 and CW2.

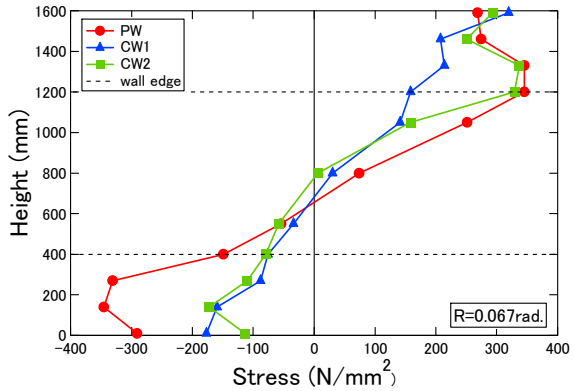

(a) Stress distribution at R=0.0067 rad.

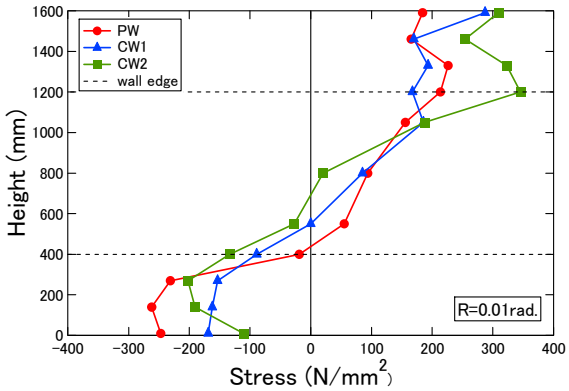

(b) Stress distribution at R=0.01 rad.

Figure 3.5 Stress distribution of column main bars

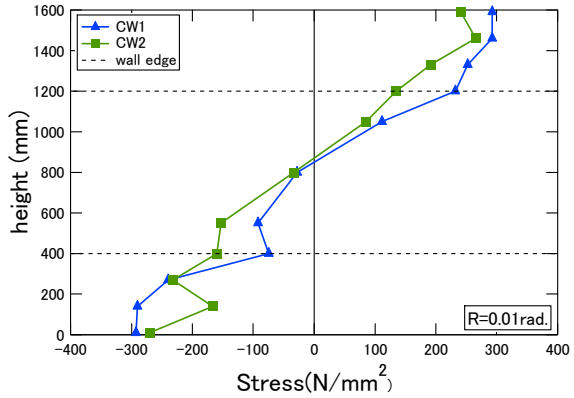

Figure 3.6 Stress distribution of steel flange

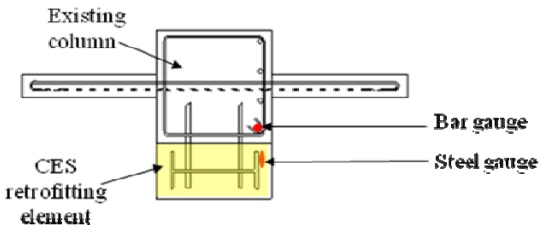

Figure 3.7 Location of strain gauges

The specimens presented very similar stress distribution (almost linear) in the middle part of the column between height of 400mm and 1200 mm. However since the specimens showed a non uniform distribution between 0-400mm and 1200-1600mm height, it is possible to infer that the specimens receive a the influence of the confinement provided by the walls as shown in Fig. 3.5.

On the other hand for specimens CW1 and CW2, in the zone between 0-400 mm and 1200-1600 mm, the stresses of the steel flange showed a uniform distribution, therefore it is possible to infer that it not receive the any confinement influence by the walls. In this sense it is possible to say that the clear height of the CES retrofitting element can be estimated as 1600 mm.

4. ULTIMATE STRENGTH EVALUATION

The bending and shear strength calculations for the specimens are shown in Table 4.1. The calculations are made using two patterns for the height of the column, 1600 mm and 800 mm respectively. For the of the shear strength of the existing column ${}_{E}Q_{su}$ the Arakawa's mean value formula was used, while the bending strength ${}_{E}Q_{mu}$ was calculated based on the formulation given by Seismic Evaluation and Retrofit (Japan Building Disaster Association, 2001).

For the CES retrofitting element, the shear strength ${}_{R}Q_{su}$ was calculated using the Standard for Structural Calculation of Steel Reinforced Concrete (AIJ, 2001), as shown in Eqn. 4.1. On the other hand the bending strength of the CES retrofitting element was calculated using the conventional superimposed strength theory with axial force N=0kN, same as the experimental conditions.

The ultimate strength of the retrofitted specimens CW1 and CW2 was calculated by the simple superposition of the strength values obtained for the existing column and the CES retrofitting element.

$$ {}_{R}Q_{su} = \left({}_{Rw}t \cdot {}_{Rw}H \cdot {}_{Rw}\sigma_{y} / \sqrt{3} + \tan\theta \cdot {}_{R}b \cdot \mu \cdot {}_{R}D \cdot {}_{R}\sigma_{c} / 2 \right) \tag{4.1} $$

${}_{Rw}t$: width of steel web (mm)
${}_{Rw}H$: depth of steel web (mm)
${}_{Rw}\sigma_{y}$: yielding strength of steel web (N/mm^2)
${}_{R}b$: width of the CES reinforcing element (mm)
${}_{R}b'$: concrete effective width (mm)
${}_{R}D$: CES retrofitting element depth (mm)
${}_{R}\sigma_{c}$: compressive strength of the CES retrofitting element (N/mm^2)
$\mu = (0.5 + {}_{R}b / {}_{R}b') \le 1.0$

Table 4.1 Ultimate strength calculations

Specimens				Without retrofit	Retrofitted	
				PW	CW1	CW2
Calculated values	Existing column	h_0=1600	${}_{E}Q_{su}$	233.8	233.9	241.2
			${}_{E}Q_{mu}$	275.5	275.5	278.5
		h_0=800	${}_{E}Q_{su}$	347.6	347.8	361.6
			${}_{E}Q_{mu}$	550.9	551.0	557.0
	CES retrofitting element	h_0=1600	${}_{R}Q_{su}$		413.1	502.3
			${}_{R}Q_{mu}$		254.1	346.6
		h_0=800	${}_{R}Q_{su}$		533.8	647.7
			${}_{R}Q_{mu}$		508.3	693.2
	Existing col. + CES retrofitting element	h_0=1600	Q_{cal1}	233.8	488.1	587.8
		h_0=800	Q_{cal2}	347.6	856.1	1009.3
		Existing Col h_0=800 Retrofitting Elem h_0=1600	Q_{cal3}	347.6	602.0	708.2
Experimental value			Q_{exp}	411.8	619.6	706.7
Experimental to calculated value ratio			Q_{exp}/Q_{cal1}	1.76	1.27	1.20
			Q_{exp}/Q_{cal2}	1.18	0.72	0.70
			Q_{exp}/Q_{cal3}	1.18	1.03	1.00

Calculations of the strength of the existing columns and the CES retrofitting element using 1600mm for both as clear height of the column (Q_{cal1}), 800mm for both as clear height of the column (Q_{cal2}), and 800mm and 1600mm for the existing column and CES retrofitting element respectively (Q_{cal3}) were

made and compared with the experimental values.

For specimen CW and CW2 the ratio $Q_{exp}/Q_{cal3}$was 1.00, indicating that it is appropriate to consider different clear height for the existing column and CES retrofitting element as expressed in previous sections.

5. CONCLUSIONS

An experimental study was conducted to evaluate the effectiveness of the CES retrofit system on columns with spandrel walls and the evaluation of their ultimate strength. Based on the test results the following conclusions can be reached.

1) Shear failure prone existing columns provided with spandrel walls, can considerably improve their seismic performance when retrofitted with CES retrofit system.

2) The CES retrofitting element when attached to existing columns with spandrel walls did not receive much influence of the confinement given by the walls, and the CES retrofitting element tend to reach the bending yielding stress at both end of the column.

3) Based on the analysis of this experiment for shear failure prone existing columns with CES retrofit system it is appropriated to consider for the calculations the inner height between the walls as the clear height for the existing column and the total height of the column as clear height for the CES retrofitting element.

4) It was verified that the ultimate strength of columns retrofitted with CES system can calculated by the superimposed strengths of the existing column and the CES retrofitting element.

REFERENCES

Taguchi, T., Kuramoto, H. et al. (2007). Development of CES Outer Frame for Retrofitting. Summaries of Technical Papers of Annual Meeting, AIJ, Vol.C-1, 1277–1278 (in Japanese).

Kuramoto, H., Takahashi, H. and Maeda, M. (2000). Feasibility study on structural performance of concrete encased steel columns using high performance fiber reinforced cementitious composites. AIJ, Summaries of Technical Papers of Annual Meeting, Vol.C-1, 1085–1088, (in Japanese).

Kuramoto, H., Adachi, T. and Kawasaki, K. (2002). Behavior of concrete encased steel composite columns using FRC. Proceedings of Workshop on Smart Structural Systems Organized for US-Japan Cooperative Research Programs on Smart Structural Systems (Auto-Adaptive Media) and Urban Earthquake Disaster Mitigation, Tsukuba, Japan, 13-26.

Architectural Institute of Japan (2001). Standards for Structural Calculation of Steel Reinforced Concrete Structures. (in Japanese)

Japan Building Disaster Association (2001), Seismic Evaluation and Retrofit for Steel Reinforced Concrete Structures. (in Japanese)